Cell Reports
Physical Science

CellPress
OPEN ACCESS

Article

Discrete chiral organic nanotubes by stacking pillar[5]arenes using covalent linkages

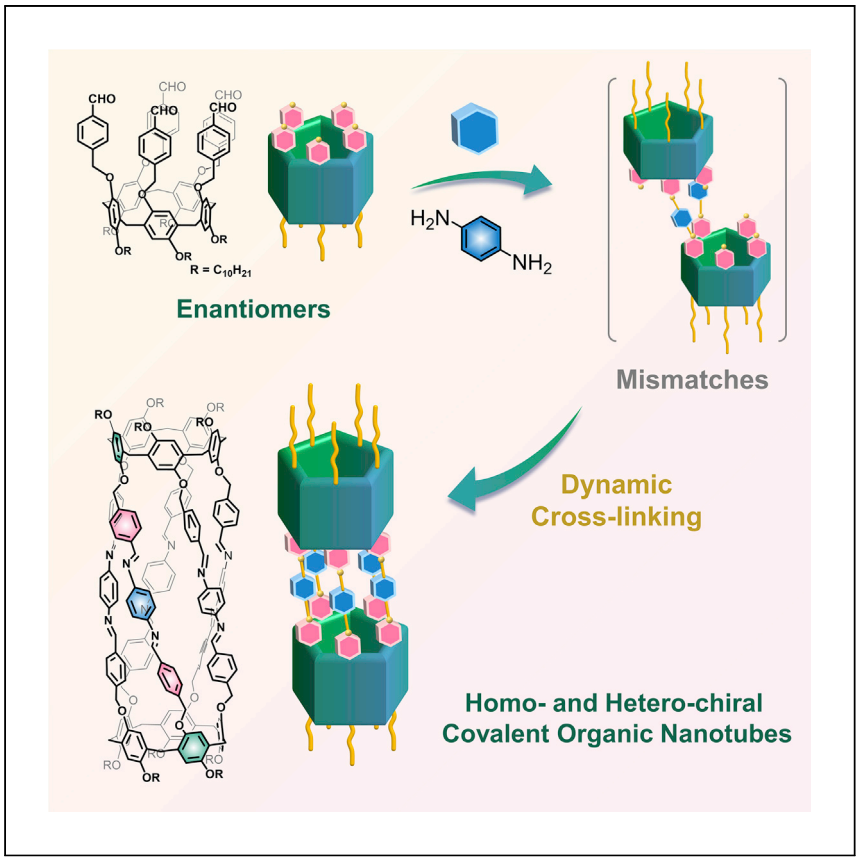

Shi and Fa et al. report covalent organic nanotubes with 5-fold symmetry by stacking two pillar-shaped macrocycles through dynamic covalent linkages. Three different chiral nanotubes are separated, providing one-dimensional channels with different chirality. When binding with guest molecules, two pillar[5]arene cavities communicate with each other, resulting in allosteric binding affinities.

Tan-Hao Shi, Shixin Fa, Yuuya Nagata, Keisuke Wada, Shunsuke Ohtani, Kenichi Kato, Tomoki Ogoshi

ogoshi@sbchem.kyoto-u.ac.jp

Highlights

Organic nanotubes are obtained by stacking pillar[5]arenes by covalent linkages

Using dynamic covalent bonds results in discrete nanotubes with 5-fold symmetry

Three different chiral nanotubes are obtained by chiral column separation

Two pillar cavities in the tube communicate with each other by allosteric effects

Shi et al., Cell Reports Physical Science 3, 101173
December 21, 2022
https://doi.org/10.1016/j.xcrp.2022.101173

Cell Reports
Physical Science

CellPress
OPEN ACCESS

Article

Discrete chiral organic nanotubes by stacking pillar[5]arenes using covalent linkages

Tan-Hao Shi,[1,5] Shixin Fa,[1,2,5] Yuuya Nagata,[3] Keisuke Wada,[1] Shunsuke Ohtani,[1] Kenichi Kato,[1] and Tomoki Ogoshi[1,4,6,7,8,*]

SUMMARY

Owing to their unique one-dimensional hollow structures, organic nanotubes have been widely explored in recent years. Covalent organic nanotubes (CONs) can be prepared by stacking building blocks, such as macrocycles, through covalent linkages. However, because of the mismatched covalent connections, controllable synthesis of the discrete CONs with clear structures, such as sidewall and chirality, is a challenging target. In this work, by coupling two pillar[5]arenes through dynamic covalent bonds, thermodynamically stable discrete CONs with 5-fold symmetry are successfully prepared. Three different chiral CONs are separated, including homo-CONs, consisting of two enantiomers (*p*R, *p*R and *p*S, *p*S), and hetero-CON, consisting of the *meso* form (*p*R, *p*S). These CONs show negative allosteric binding affinities toward guest molecules, which are not observed in individual pillar[5]arenes.

INTRODUCTION

Nanotubes are one-dimensional hollow tubular architectures. Owing to their wealth of potential applications in science and technology, nanotubes have attracted scientists for decades.[1,2] However, due to the limitations in synthetic methods, the preparation of nanotubes with specific structures (such as composition, diameter, and chirality) is extremely difficult. For example, controlling these specific structures in synthesizing single-walled carbon nanotubes has been a challenge to scientists for years.[3,4]

Compared with carbon nanotubes, structures of organic nanotubes are easy to be controlled because of their high functionality.[2,5–10] Organic nanotubes have been used in molecular recognition,[6–9] ion channels,[11–13] and conductive materials.[14,15] They were generally constructed by non-covalent assembly (Figure 1A). However, because the architectures are maintained by weak non-covalent connections, these tubular structures are fragile. To construct robust organic nanotubes, covalent cross-linking was applied.[16–21] Nevertheless, during the multipoint cross-linking, perfect matches are difficult because the reactive sites can remain intact or be mismatched (Figure 1B). Therefore, due to the uncross-linking and mismatches, controllable synthesis of the covalent organic nanotubes (CONs) with these specific structures has remained challenging.[22–24]

In the present study, pillar[5]arenes[25,26] were chosen as materials of CONs because their preorganized and symmetric pillar structures enabled them to be adequate building blocks for nanotubes; for example, non-covalent bond nanotubes were previously prepared based on pillar[5]arenes.[27–30] To obtain discrete CONs, the rim-differentiated pillar[5]arene **1** (Figure 1C), which have reactive aldehydes and

[1]Department of Synthetic Chemistry and Biological Chemistry, Graduate School of Engineering, Kyoto University, Katsura, Nishikyo-ku, Kyoto 615-8510, Japan

[2]School of Chemistry and Chemical Engineering, Northwestern Polytechnical University, Xi'an, Shaanxi 710072, P.R. China

[3]WPI Institute for Chemical Reaction Design and Discovery, Hokkaido University, Kita 21 Nishi 10, Kita-ku, Sapporo 001-0021, Japan

[4]WPI Nano Life Science Institute (WPI-NanoLSI), Kanazawa University, Kakuma-machi, Kanazawa, Ishikawa 920-1192, Japan

[5]These authors contributed equally

[6]Twitter: @ogoshi_lab

[7]Twitter: @ogoshitomoki

[8]Lead contact

*Correspondence: ogoshi@sbchem.kyoto-u.ac.jp

https://doi.org/10.1016/j.xcrp.2022.101173

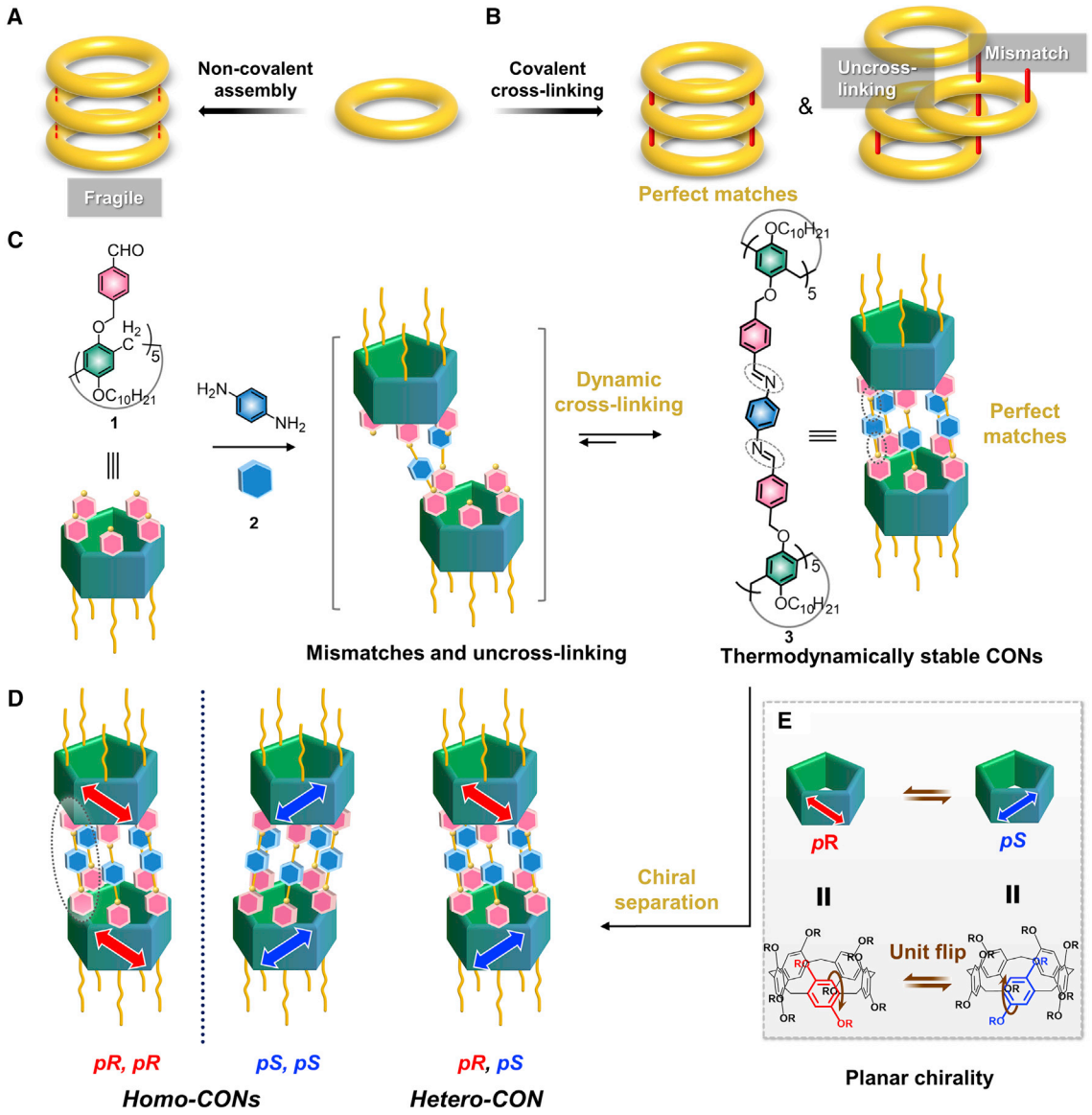

Figure 1. Organic nanotubes and synthetic strategy

(A) Non-covalent organic nanotubes.

(B) Covalent organic nanotubes (CONs) and difficulties in their synthesis because of uncross-linking and mismatch.

(C) Preparation of thermodynamically stable CONs from pillar[5]arenes using dynamic cross-linking.

(D) Discrete CONs based on pillar[n]arenes with different chiralities.

(E) Planar chirality of pillar[5]arenes.

inactive alkyl groups installed separately on the two rims, were used. Dimerization of **1** will produce the discrete CONs in 5-fold symmetry. In this procedure, 10 cross-linking points were required to be perfectly matched. To avoid the mistakes in the process, diamines **2** were used as linkages to cross-link the pillar[5]arene aldehydes through dynamic imine bonds.[31,32] The mismatched and uncross-linked sites will be repaired automatically, furnishing thermodynamically stable discrete chiral CONs **3** with 5-fold symmetry (Figure 1C).

Pillar[n]arenes have two stable planar-chiral conformers (Figure 1E) because of the directional substitutions on the phenyl units.[33,34] These two stable conformers of

pillar[n]arenes can interconvert through unit flip. Here, the unit flip of pillar[5]arene building blocks is inhibited by the cross-linking, and three different chiral CONs are separated, including homo-CONs, consisting of two enantiomers (*p*R, *p*R and *p*S, *p*S), and hetero-CON, consisting of the meso form (*p*R, *p*S) (Figure 1D). Although chiral nanotubes have been constructed through non-covalent interactions,[6,10,30] the synthesis of discrete chiral CONs has never been reported. Thanks to the robust CONs, we can separate these different chiral isomers and investigate their host-guest properties. In their host-guest interaction, the two pillar[5]arenes communicated with each other through the one-dimensional channel. The first binding adversely affected the second binding process through an allosteric effect, which was not observed in individual pillar[5]arenes and the pillar[5]arene-based non-covalent nanotubes.[27,30]

RESULTS AND DISCUSSION

Design and synthesis of CONs

Rim-differentiated pillar[5]arene **1**, which possesses aromatic aldehydes on one edge and long alkyl chains on the other, was synthesized (details in supplemental experimental procedures; Figures S28–S35).[35–37] CON formation was conducted between **1** (1 equiv) and benzene-1,4-diamine **2** (2.5 equiv) (Figure 2A). After reaction for 36 h at 60°C in chloroform, the proton signals of **1** disappeared, and two new sets of peaks emerged. No obvious changes in the ^{1}H nuclear magnetic resonance (NMR) spectra were observed with a longer reaction time (48 h) (Figure S1), indicating a complete reaction. The products were then purified by recycling gel permeation chromatography (GPC) to remove mismatched by-products (i.e., polymer and non-linear oligomers) (Figures S2 and S3). The CONs with two sets of sharp ^{1}H NMR peaks, which corresponded to the homo- and hetero-isomers of CONs **3** (*vide infra*), were obtained in 48% yield (Figures 2C and S4). Since 10 new C=N bonds were formed in the synthesis, 48% yield implied that each new bond formation was correctly performed in 93% yield, indicating the high efficiency of the dynamic bond strategy. The diastereomeric ratio (*dr*) values of homo-CON to hetero-CON were determined to be 3.4 from the integral ratios of H_5 of homo- and hetero-CONs in ^{1}H NMR spectra (Figure S7). When the homo- and hetero-CONs are generated in a 1:1 ratio, the *dr* value is 1. The higher *dr* value indicated that the homo-CONs were generated selectively under the reaction condition. The reaction was optimized with different temperatures, solvents, and additives (details in Table S1). With appropriate guest molecules, such as 1,2-dicyanoethane, the selectivity increased (*dr* = 10.3); this was probably facilitated through thermodynamical control (*vide infra*). And with catalytic trifluoroacetic acid, the yield of the CONs can be increased to 65%, that is, 96% for each C=N bond (Figure 2A; Table S1). The structures of CONs were modulated by using different diamine as linkers, and when benzidine was used, stable CONs with longer lengths were obtained (details in Figures S8, S24–S26, and S40–S43). The reduction of the imine bonds was achieved using $NaBH_4$, but the obtained product was easily oxidized during purification (Figure S27).

Chiral separation of the CONs was then achieved using recycling chiral high-performance liquid chromatography (HPLC), and three fractions (**F1**, **F2**, and **F3**) were collected (Figure 2B). **F1** and **F3** had identical ^{1}H NMR spectra (Figure 2E), which contained the main peaks in the ^{1}H NMR of the mixture (Figure 2C). The minor peaks in the spectrum of the mixture were from **F2** (Figure 2D). In all the ^{1}H NMR spectra, H_1, H_2, H_5, and H_6 exhibited clear singlets, while H_3 and H_4 exhibited doublets, indicating that the structures of the CONs were symmetrical. The splitting of H_c

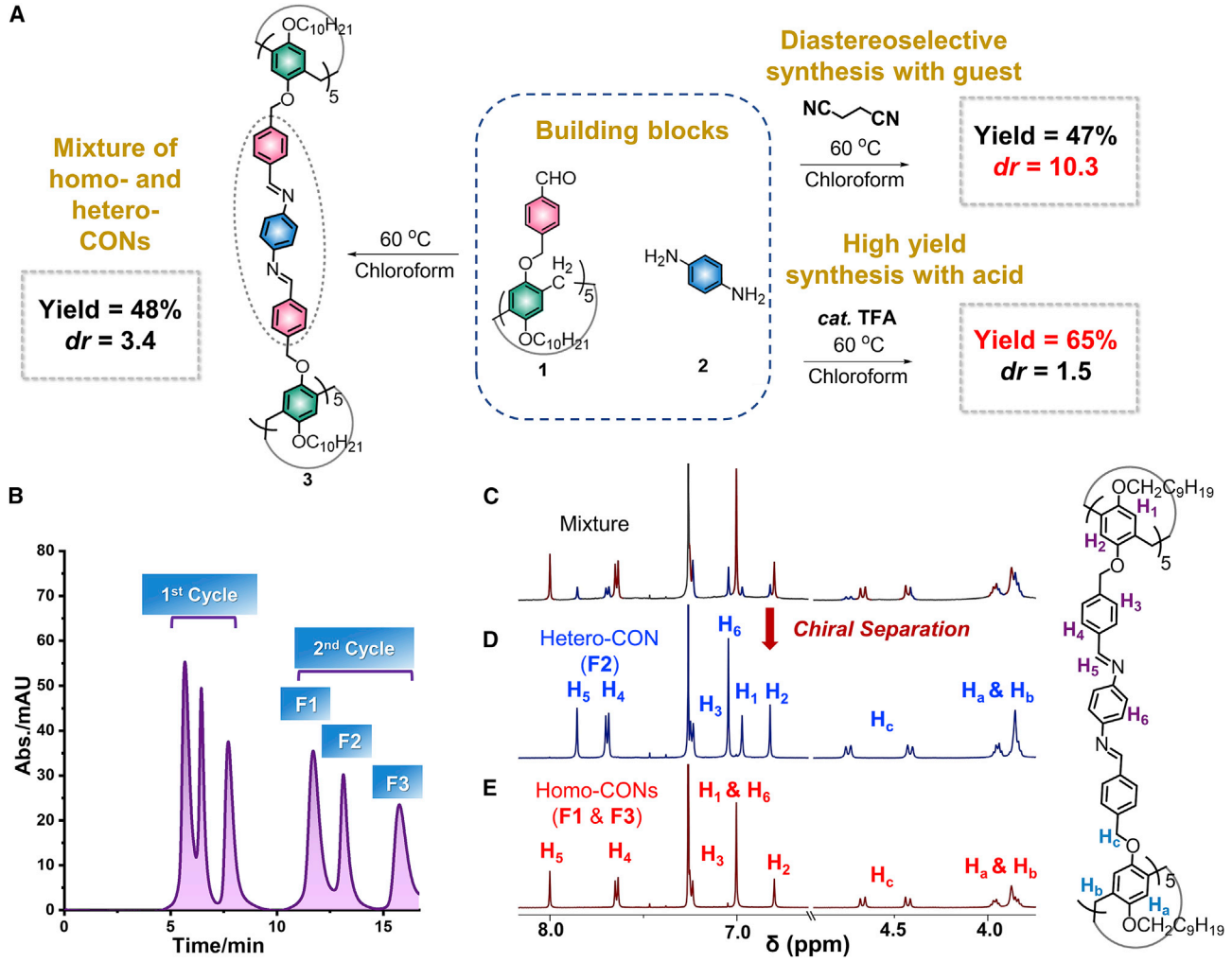

Figure 2. Synthesis, separation, and characterization of CONs

(A) Preparation of CONs from pillar[5]arenes using dynamic covalent bonds.

(B) Chiral separation of CON isomers (IA column, chloroform/*n*-hexane/triethylamine = 4/6/0.01; flow rate: 5 mL/min).

(C–E) Partial ^{1}H NMR spectra (25°C, 500 MHz, $CDCl_3$) of CONs **3**: (C) mixture before chiral separation, (D) hetero-CON **F2**, and (E) homo-CONs **F1** and **F3** after chiral separation.

indicated that the two protons in the same methylene group were diastereotopic,[38] indicating that the flipping of the units was restricted (detailed NMR spectra in Figures S36–S39). In the high-resolution MALDI mass spectra, all the separated products exhibited the same mass peaks, which corresponded to $[M]^+$ of the CONs (Figure S24).

Optical properties of CONs

The UV-visible (UV-vis) and circular dichroism (CD) spectra were then obtained to investigate the stereochemistry of the different isomers (Figure 3A). In the UV-vis spectra, the three compounds all exhibited similar patterns (Figure S5), indicating that they had similar structures. Absorption bands at approximately 290 and 351 nm were ascribed to the π–π* transitions of the benzenes in the pillar[5]arene backbones and the n–π*/π–π* transitions of the linkers, respectively.[39,40] **F1** and **F3** were mirror images, and **F2** showed no CD signals. Therefore, **F1** and **F3** were determined to be enantiomeric homo-CONs (*p*R, *p*R and *p*S, *p*S) and **F2**

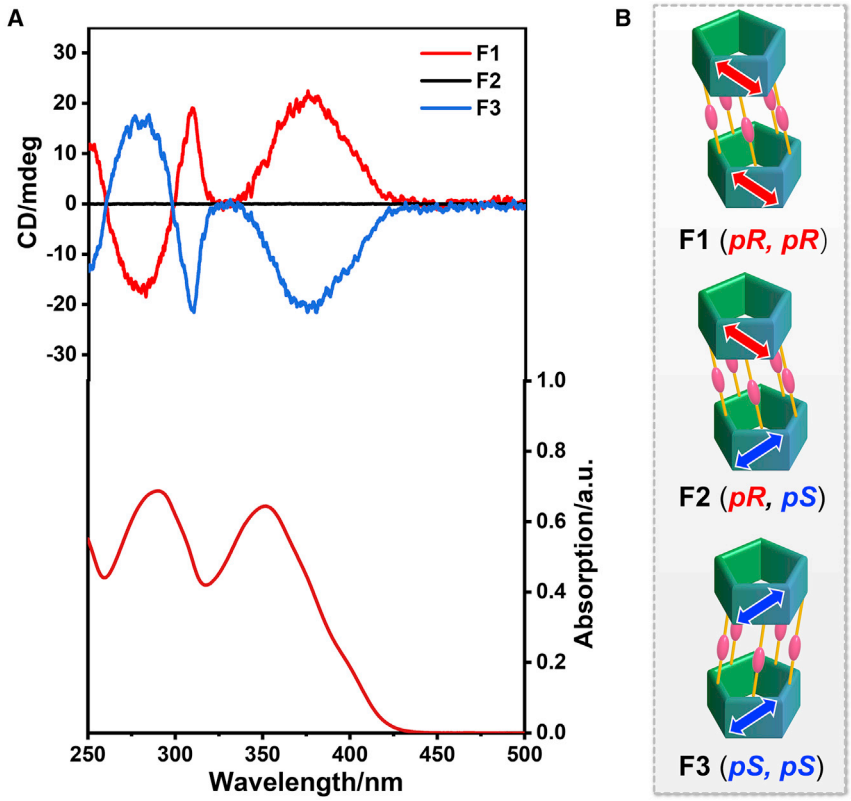

Figure 3. Optical spectra and chirality of CONs

(A) UV-vis spectrum (bottom) of **F1** and CD spectra (top) of different CONs (solvent: chloroform; concentration: 5×10^{-5} M).

(B) Schematic illustration of CONs with different chirality.

was a meso hetero-CON (*p*R, *p*S) (Figure 3B). Considering that **F1** exhibited positive Δε values at approximately 310 nm, from the π–π* transitions of the benzenes in the pillar[5]arene backbones, the structure of the compound was (*p*R, *p*R).[29,41] Correspondingly, the mirror imaged **F3** was (*p*S, *p*S). The CD signals at approximately 375 nm came from the linkers, indicating that the cyclized linkers also provided a chiral environment. Because of unit swing, the CD intensities of individual pillar[n]arenes generally decrease with increasing temperature.[42] However, with changing temperatures, the CD intensities of the CONs hardly changed (Figure S6), indicating that the backbones were rigid due to the robust CON structures.

Structures and mechanism

The structures of the CONs were elucidated by theoretical calculations using ORCA 4.2.0[43] with the semiempirical GFN2-xTB method[44] and the SMD solvation model[45] (chloroform) (Figures 4, S17, and S18). The results indicated that two pillar[5]arenes were connected by a pair of imine bonds. The energy of the homo-CON was 20 kJ/mol lower than that of the hetero-CON, indicating that selective formation of the homo-CON was modulated thermodynamically.

The proposed mechanism for the selectivity observed for the homo- and hetero-CONs is shown in Figure 5. (1) After introducing the first linker, CON precursors with different chiralities were formed. (2) Precursors with different chiralities were able to interconvert through unit flip or dynamic covalent bonds. (3) More linkers

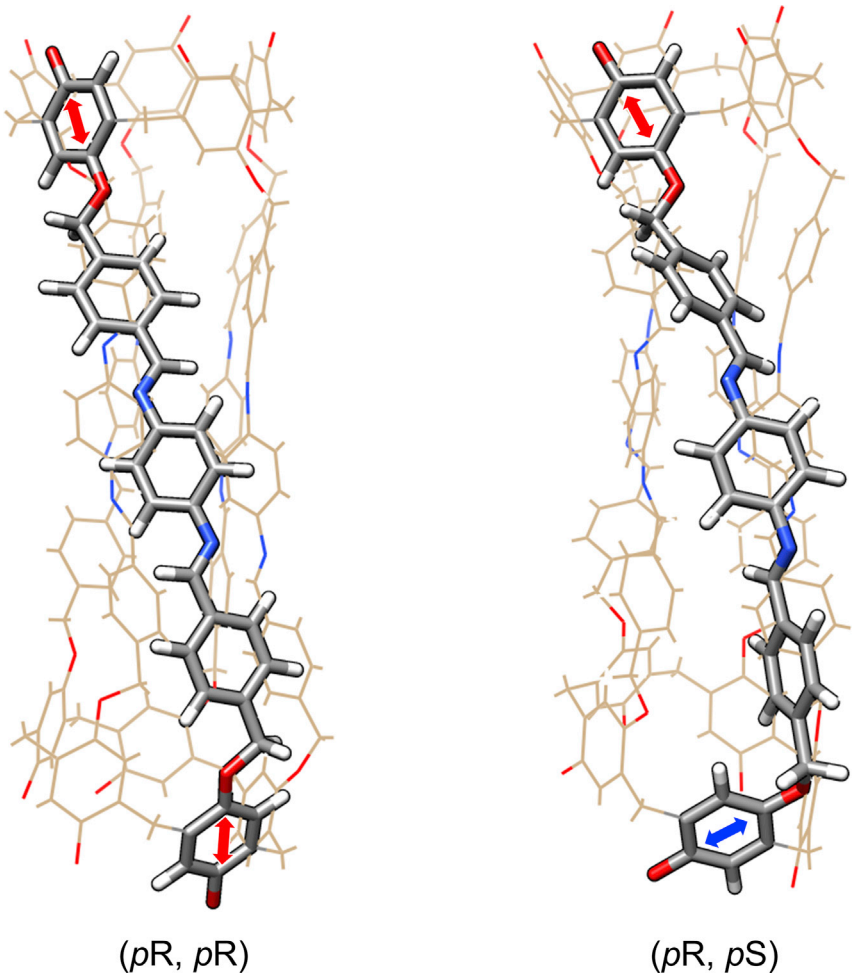

Figure 4. Calculated structures of the homo- and hetero-CONs

The long alkyl chains were hidden for clarifying. Different chiralities are marked as red (*p*R) and blue (*p*S) arrows.

were gradually incorporated into the dimer precursors, and finally, CONs were formed. (4) The CONs with different chiralities were all stable and did not interconvert. Because when CONs with different *dr* values were heated in chloroform, even with 1,2-dicyanoethane and catalytic amount of TFA, the *dr* values did not change (Figures S9–S12). Therefore, the selectivity was determined before the CON formation. Homo-precursors (*p*R, *p*R and *p*S, *p*S) were more thermodynamically favored, leading to the formation of a higher proportion of homo-CONs, compared with hetero-CON, in the preparation (Table S1, entry 1). With appropriate guests, such as 1,2-dicyanoethane, the equilibrium toward homo-precursors was facilitated through thermodynamic control, and a higher *dr* value was obtained (Table S1, entry 14), probably because homo-CONs had higher affinity toward the guest molecules than the hetero-CON had (*vide infra*).

Host-guest properties

Because the binding between pillar[5]arenes and 1,2-dicyanoethane is strong and exchanges slowly in the NMR timescale, the complexation between the CONs and guests can be easily monitored through ^{1}H NMR spectra.[26] Therefore, 1,2-dicyanoethane was used as a guest to evaluate the binding properties of the homo-CONs (Figure 6A). During

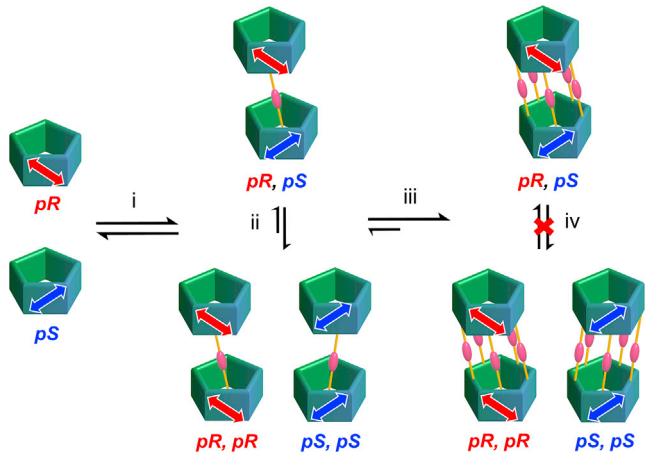

Figure 5. Proposed mechanism for the selectivity in the CON preparation

Different chiralities are marked as red (*p*R) and blue (*p*S) arrows. Imine bonds are represented as pink ellipsoid.

the ^{1}H NMR titration, a slow exchange of complexation was expectedly observed. When more than 0.2 equiv guest molecule was added, two new sets of peaks emerged ($H_{x\text{-}com1}$, blue peaks), which were attributed to the two pillar[5]arene cavities after the first binding (**complex 1** in Figure 6C). **Complex 1** is non-symmetrical, and one set of peaks was shifted downfield because of deshielding after complexation, while the other set shifted negligibly because of the empty cavity. When more than 0.4 equiv guest was added, another set of peaks emerged ($H_{x\text{-}com2}$, orange peaks), which arose from the second binding process (**complex 2** in Figure 6C). **Complex 2** is symmetrical; therefore, only one set of peaks was generated. When 3.0 equiv guest was added, only the $H_{x\text{-}com2}$ peaks remained, suggesting that the channel was saturated. The relative ratios of different species during the titration are summarized in Figure 6B. With the addition of guest, the ratio of host CON gradually decreased, and the ratio of **complex 2** gradually increased. The ratio of **complex 1** first increased and reached a maximum at 1.0 equiv and then decreased to zero at 3.0 equiv. Surprisingly, the binding properties of the two pillar[5]arene cavities were different. The binding constants for the two steps were $K_1 = (1.73 \pm 0.07) \times 10^4$ M^{-1} and $K_2 = (1.18 \pm 0.15) \times 10^4$ M^{-1} (Figure S15). The binding constant of the second binding was smaller than that of the first binding, implying a negative allosteric effect[46–48] and the formation of non-symmetrical **complex 1**. The first binding changed the conformation of the empty cavity in **complex 1**, resulting in the negative allosteric effect (Figures S17 and S19). Consequently, the second binding was adversely affected by the first binding process (Table S2; Figure S21).

The hetero-CON showed a similar complexation process (Figures S13 and S14) and allosteric effect (Table S2; Figures S18 and S20) as in the homo-CON. Two binding constants for the two steps were $K_1 = (1.65 \pm 0.08) \times 10^4$ M^{-1} and $K_2 = (3.94 \pm 0.42) \times 10^3$ M^{-1} (Figure S16). The homo-CONs had a larger binding affinity ($K_{homo} = 2.04 \times 10^8$ $M^{-2} > K_{hetero} = 0.65 \times 10^8$ M^{-2}; $K = K_1 \times K_2$) with 1,2-dicyanoethane, accounting for, to some extent, the selective formation of homo-CONs in the presence of 1,2-dicyanoethane (Figure 2A).

The addition of 1,2-dicyanoethane into a chloroform solution of (*p*S, *p*S)-CON resulted in a gradual increase in the intensity of the CD peak at a lower wavelength (310 nm), which was attributed to the pillar[5]arene moiety (Figures S22 and S23). This result suggested that the insertion of guests further limited the movement of

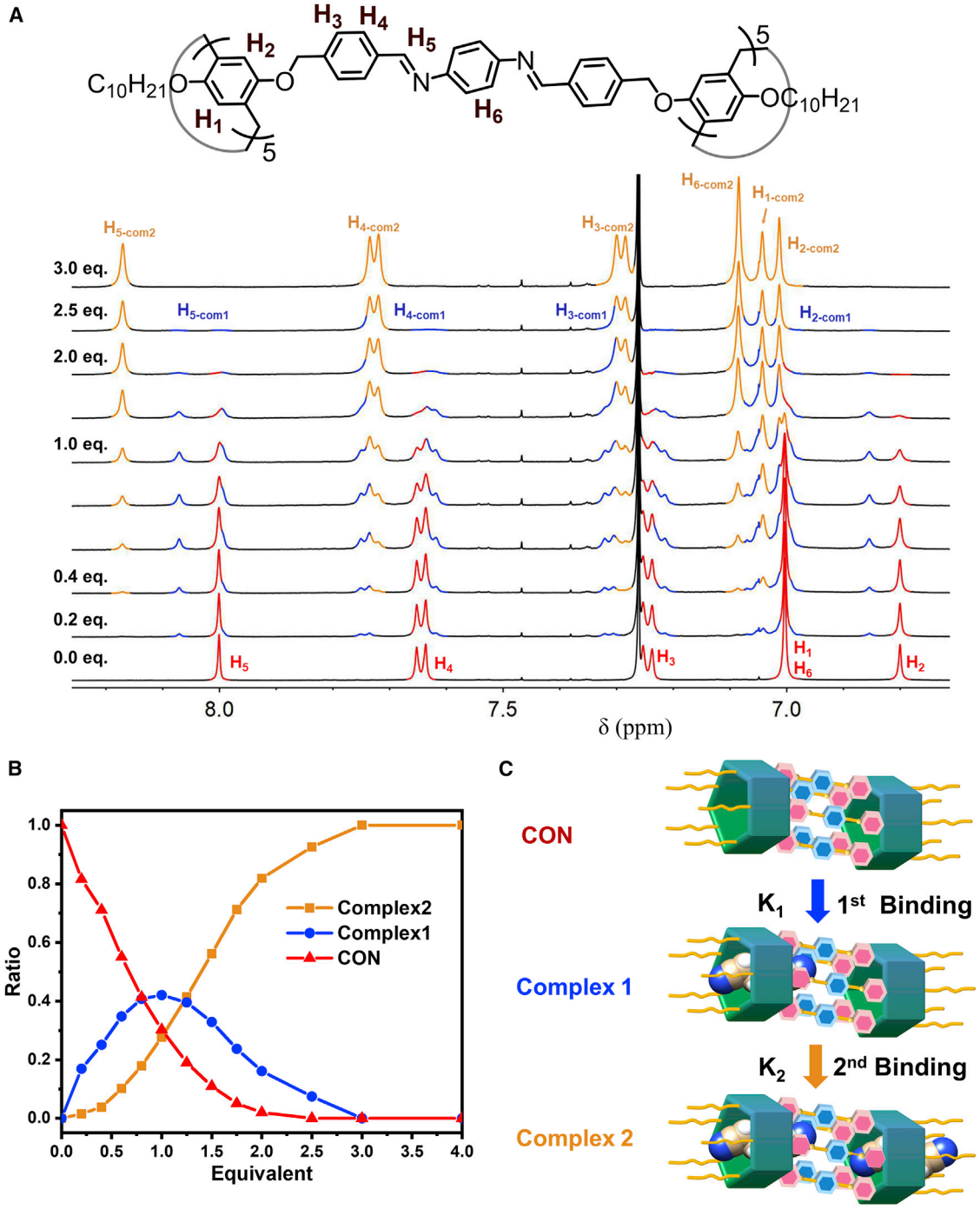

Figure 6. Host-guest property of CONs

(A) Schematic representation showing the protons in CONs and partial ^{1}H NMR spectra (25°C, 500 MHz, $CDCl_3$) of the homo-CONs with 1,2-dicyanoethane (0.0–3.0 equiv).

(B) Changes in ratios of the homo-CONs, **complex 1**, and **complex 2** with 1,2-dicyanoethane (0.0–4.0 equiv).

(C) Schematic illustration of the two binding events.

the pillar[5]arenes.[29] At the same time, a gradual decrease in the CD intensity of the peak at a higher wavelength (375 nm), which was attributed to the linkers, was also observed. It suggested that the conformations of the self-adaptive linkers changed to accommodate the guest, resulting in a decrease in the CD intensity.

In conclusion, by repairing the mismatched and uncross-linked sites via dynamic covalent bonds, two pillar[5]arenes were perfectly matched through 10 point intermolecular cross-linking, resulting in thermodynamically stable CONs with 5-fold symmetry. Previous studies have connected one of the benzenes in pillar[5]arenes via covalent bonds and constructed one-dimensional channel structures.[33] However, further cross-linking to construct nanotubes led to mismatches, resulting in amorphous products.[49]

The obtained CONs were further separated to give homo-CONs (*p*R, *p*R and *p*S, *p*S) and a hetero-CON (*p*R, *p*S), providing one-dimensional channels with different chiral environments. The homo/hetero selectivity in the synthesis could be modulated using guests, and the *dr* value was increased to 10.3 when 1,2-dicyanoethane guest was used. The two pillar[5]arenes in the CONs communicated with each other through the one-dimensional channel via negative allosteric effects. The CONs provided different chiral environments and bound guests distinctly. Therefore, these CONs can function as tubular hosts and have the potential for supramolecular applications, such as in chiral sensing and transportation.

This method will be a practical way to construct CONs from pillar[n]arenes. For example, when using different feed ratios of pillar[5]arenes to linker molecules, CONs with different lengths, such as trimer, tetramer, and polymer, can be synthesized controllably. Moreover, based on rim-differentiated pillar[6]arene, which was recently reported,[50] CONs with larger diameters can be achieved. We hope that this protocol will pave the way for the synthesis of new class of CONs based on pillar[n]arenes with controllable chirality, diameters, and lengths.

EXPERIMENTAL PROCEDURES

Resource availability

Lead contact

Further information and requests for resources should be directed to and will be fulfilled by the lead contact, Tomoki Ogoshi (ogoshi@sbchem.kyoto-u.ac.jp).

Materials availability

All materials generated in this study are available from the lead contact without restriction.

Data and code availability

The authors declare that the data supporting the findings of this study are available within the article and the supplemental information. All other data are available from the lead contact upon reasonable request.

Methods

See the supplemental experimental procedures for full details of synthesis, characterization, and analysis.

SUPPLEMENTAL INFORMATION

Supplemental information can be found online at https://doi.org/10.1016/j.xcrp.2022.101173.

ACKNOWLEDGMENTS

This work was supported by JSPS KAKENHI, Japan, grant numbers JP15H00990, JP17H05148, JP18H04510, and JP20H04670 (Scientific Research on Innovative Areas, T.O.); JP19H00909 and JP22H00334 (Scientific Research (A), T.O.); JP21K14612 (Early-Career Scientists, S.F.); JP21H01924 (Scientific Research (B), Y.N.); JST CREST, Japan, grant number JPMJCR18R3 (T.O.); JST ERATO, Japan, grant number JPMJER1903 (Y.N.); and the MEXT World Premier International Research Center Initiative (WPI), Japan. We thank Victoria Muir, PhD, from Edanz (https://jp.edanz.com/ac) for editing a draft of this manuscript. We thank Dr. Xin Geng from Zhengzhou University for editing the figures of this manuscript.

AUTHOR CONTRIBUTIONS

Conceptualization, T.-H.S., S.F., and T.O.; methodology, T.-H.S., S.F., and T.O.; investigation, T.-H.S., S.F., Y.N., K.W., and T.O.; writing – original draft, T.-H.S. and T.O.; writing – review & editing, T.-H.S., S.F., S.O., K.K., and T.O.; supervision, T.O.

DECLARATION OF INTERESTS

The authors declare no competing interests.

Received: September 2, 2022
Revised: November 1, 2022
Accepted: November 9, 2022
Published: December 1, 2022

REFERENCES

1. Dresselhaus, M., Dresselhaus, G., and Avouris, P. (2001). Carbon Nanotubes: Synthesis, Properties and Applications (Springer).

2. Balbo Block, M.A., Kaiser, C., Khan, A., and Hecht, S. (2005). Discrete organic nanotubes based on a combination of covalent and non-covalent approaches. Top. Curr. Chem. *245*, 89–150. https://doi.org/10.1007/b98167.

3. Iijima, S. (1991). Helical microtubules of graphitic carbon. Nature *354*, 56–58. https://doi.org/10.1038/354056a0.

4. Omachi, H., Nakayama, T., Takahashi, E., Segawa, Y., and Itami, K. (2013). Initiation of carbon nanotube growth by well-defined carbon nanorings. Nat. Chem. *5*, 572–576. https://doi.org/10.1038/nchem.1655.

5. Shimizu, T., Masuda, M., and Minamikawa, H. (2005). Supramolecular nanotube architectures based on amphiphilic molecules. Chem. Rev. *105*, 1401–1443. https://doi.org/10.1021/cr030072j.

6. Bong, D.T., Clark, T.D., Granja, J.R., and Ghadiri, M.R. (2001). Self-assembling organic nanotubes. Angew. Chem. Int. Ed. Engl. *40*, 988–1011. https://doi.org/10.1002/1521-3773(20010316)40:6<988::AID-ANIE9880>3.0.CO;2-N.

7. Shimizu, T. (2008). Molecular self-assembly into one-dimensional nanotube architectures and exploitation of their functions. Bull. Chem. Soc. Jpn. *81*, 1554–1566. https://doi.org/10.1246/bcsj.81.1554.

8. Kameta, N., Minamikawa, H., and Masuda, M. (2011). Supramolecular organic nanotubes: how to utilize the inner nanospace and the outer space. Soft Matter *7*, 4539–4561. https://doi.org/10.1039/C0SM01559H.

9. Shimizu, T., Ding, W., and Kameta, N. (2020). Soft-matter nanotubes: a platform for diverse functions and applications. Chem. Rev. *120*, 2347–2407. https://doi.org/10.1021/acs.chemrev.9b00509.

10. Chamorro, P.B., and Aparicio, F. (2021). Chiral nanotubes self-assembled from discrete non-covalent macrocycles. Chem. Commun. *57*, 12712–12724. https://doi.org/10.1039/D1CC04968B.

11. Helsel, A.J., Brown, A.L., Yamato, K., Feng, W., Yuan, L., Clements, A.J., Harding, S.V., Szabo, G., Shao, Z., and Gong, B. (2008). Highly conducting transmembrane pores formed by aromatic oligoamide macrocycles. J. Am. Chem. Soc. *130*, 15784–15785. https://doi.org/10.1021/ja807078y.

12. Montenegro, J., Ghadiri, M.R., and Granja, J.R. (2013). Ion channel models based on self-assembling cyclic peptide nanotubes. Acc. Chem. Res. *46*, 2955–2965. https://doi.org/10.1021/ar400061d.

13. Roy, A., Joshi, H., Ye, R., Shen, J., Chen, F., Aksimentiev, A., and Zeng, H. (2020). Polyhydrazide-based organic nanotubes as efficient and selective artificial iodide channels. Angew. Chem. Int. Ed. Engl. *59*, 4806–4813. https://doi.org/10.1002/anie.201916287.

14. Hill, J.P., Jin, W., Kosaka, A., Fukushima, T., Ichihara, H., Shimomura, T., Ito, K., Hashizume, T., Ishii, N., and Aida, T. (2004). Self-assembled hexa-peri-hexabenzocoronene graphitic nanotube. Science *304*, 1481–1483. https://doi.org/10.1126/science.1097789.

15. Yamamoto, Y., Fukushima, T., Suna, Y., Ishii, N., Saeki, A., Seki, S., Tagawa, S., Taniguchi, M., Kawai, T., and Aida, T. (2006). Photoconductive coaxial nanotubes of molecularly connected electron donor and acceptor layers. Science *314*, 1761–1764. https://doi.org/10.1126/science.1134441.

16. Harada, A., Li, J., and Kamachi, M. (1993). Synthesis of a tubular polymer from threaded cyclodextrins. Nature *364*, 516–518. https://doi.org/10.1038/364516a0.

17. Xu, Y., Smith, M.D., Geer, M.F., Pellechia, P.J., Brown, J.C., Wibowo, A.C., and Shimizu, L.S. (2010). Thermal reaction of a columnar assembled diacetylene macrocycle. J. Am. Chem. Soc. *132*, 5334–5335. https://doi.org/10.1021/ja9107066.

18. Hsu, T.J., Fowler, F.W., and Lauher, J.W. (2012). Preparation and structure of a tubular addition polymer: a true synthetic nanotube. J. Am. Chem. Soc. *134*, 142–145. https://doi.org/10.1021/ja209792f.

19. Maeda, K., Hong, L., Nishihara, T., Nakanishi, Y., Miyauchi, Y., Kitaura, R., Ousaka, N., Yashima, E., Ito, H., and Itami, K. (2016). Construction of covalent organic nanotubes by light-induced cross-linking of diacetylene-based helical polymers. J. Am. Chem. Soc. *138*,

11001–11008. https://doi.org/10.1021/jacs.6b05582.

20. Rondeau-Gagné, S., Néabo, J.R., Desroches, M., Larouche, J., Brisson, J., and Morin, J.F. (2013). Topochemical polymerization of phenylacetylene macrocycles: a new strategy for the preparation of organic nanorods. J. Am. Chem. Soc. *135*, 110–113. https://doi.org/10.1021/ja3116422.

21. Koner, K., Karak, S., Kandambeth, S., Karak, S., Thomas, N., Leanza, L., Perego, C., Pesce, L., Capelli, R., Moun, M., et al. (2022). Porous covalent organic nanotubes and their assembly in loops and toroids. Nat. Chem. *14*, 507–514. https://doi.org/10.1038/s41557-022-00908-1.

22. Neuhaus, P., Cnossen, A., Gong, J.Q., Herz, L.M., and Anderson, H.L. (2015). A molecular nanotube with three-dimensional π-conjugation. Angew. Chem. Int. Ed. Engl. *54*, 7344–7348. https://doi.org/10.1002/anie.201502735.

23. Haver, R., and Anderson, H.L. (2018). Synthesis and properties of porphyrin nanotubes. Helv. Chim. Acta *102*, e1800211. https://doi.org/10.1002/hlca.201800211.

24. Mao, L.-L., Xiao, H., Zhao, J.-Q., Diao, Z., Zhou, W., Li, H., Tung, C.-H., Wu, L.-Z., and Cong, H. (2022). Synthesis of finite molecular nanotubes by connecting axially functionalized macrocycles. CCS Chem. https://doi.org/10.31635/ccschem.022.202101728.

25. Ogoshi, T., Kanai, S., Fujinami, S., Yamagishi, T.A., and Nakamoto, Y. (2008). *para*-Bridged symmetrical pillar[5]arenes: their lewis acid catalyzed synthesis and host–guest property. J. Am. Chem. Soc. *130*, 5022–5023. https://doi.org/10.1021/ja711260m.

26. Ogoshi, T., Yamagishi, T.A., and Nakamoto, Y. (2016). Pillar-shaped macrocyclic hosts pillar[n]arenes: new key players for supramolecular chemistry. Chem. Rev. *116*, 7937–8002. https://doi.org/10.1021/acs.chemrev.5b00765.

27. Fa, S., Sakata, Y., Akine, S., and Ogoshi, T. (2020). Non-covalent interactions enable the length-controlled generation of discrete tubes capable of guest exchange. Angew. Chem. Int. Ed. Engl. *59*, 9309–9313. https://doi.org/10.1002/anie.201916515.

28. Kato, K., Ohtani, S., Fa, S., and Ogoshi, T. (2021). Discrete and continuous one-dimensional channels based on pillar[n]arenes. Bull. Chem. Soc. Jpn. *94*, 2319–2328. https://doi.org/10.1246/bcsj.20210243.

29. Fa, S., Adachi, K., Nagata, Y., Egami, K., Kato, K., and Ogoshi, T. (2021). Pre-regulation of the planar chirality of pillar[5]arenes for preparing discrete chiral nanotubes. Chem. Sci. *12*, 3483–3488. https://doi.org/10.1039/D1SC00074H.

30. Wan, X., Li, S., Tian, Y., Xu, J., Shen, L.-C., Zuilhof, H., Zhang, M., and Sue, A.C.-H. (2022). Twisted pentagonal prisms: Ag_nL_2 metal-organic pillars. Chem *8*, 2136–2147. https://doi.org/10.1016/j.chempr.2022.04.001.

31. Belowich, M.E., and Stoddart, J.F. (2012). Dynamic imine chemistry. Chem. Soc. Rev. *41*, 2003–2024. https://doi.org/10.1039/C2CS15305J.

32. Zhang, W., Chen, L., Dai, S., Zhao, C., Ma, C., Wei, L., Zhu, M., Chong, S.Y., Yang, H., Liu, L., et al. (2022). Reconstructed covalent organic frameworks. Nature *604*, 72–79. https://doi.org/10.1038/s41586-022-04443-4.

33. Fa, S., Kakuta, T., Yamagishi, T.A., and Ogoshi, T. (2019). Conformation and planar chirality of pillar[n]arenes. Chem. Lett. *48*, 1278–1287. https://doi.org/10.1246/cl.190544.

34. Strutt, N.L., Zhang, H., Schneebeli, S.T., and Stoddart, J.F. (2014). Amino–functionalized pillar[5]arene. Chem. Eur. J. *20*, 10996–11004. https://doi.org/10.1002/chem.201403235.

35. Ding, J., Chen, J., Mao, W., Huang, J., and Ma, D. (2017). A new synthetic method for non-symmetric pillar[5]arenes with simple isolation and improved yield. Org. Biomol. Chem. *15*, 7894–7897. https://doi.org/10.1039/C7OB02013A.

36. Guo, M., Wang, X., Zhan, C., Demay-Drouhard, P., Li, W., Du, K., Olson, M.A., Zuilhof, H., and Sue, A.C.-H. (2018). Rim-differentiated C_5-symmetric tiara-pillar[5]arenes. J. Am. Chem. Soc. *140*, 74–77. https://doi.org/10.1021/jacs.7b10767.

37. Du, K., and Sue, A.C.-H. (2019). The trouble with five: new synthetic strategies toward C_5 -symmetric pillar[5]arenes and beyond. Synlett *30*, 2209–2215. https://doi.org/10.1055/s-0037-1611921.

38. Ogoshi, T., Kitajima, K., Aoki, T., Fujinami, S., Yamagishi, T.A., and Nakamoto, Y. (2010). Synthesis and conformational characteristics of alkyl-substituted pillar[5]arenes. J. Org. Chem. *75*, 3268–3273. https://doi.org/10.1021/jo100273n.

39. Ogoshi, T., Shiga, R., Yamagishi, T.A., and Nakamoto, Y. (2011). Planar-chiral pillar[5]arene: chiral switches induced by multiexternal stimulus of temperature, solvents, and addition of achiral guest molecule. J. Org. Chem. *76*, 618–622. https://doi.org/10.1021/jo1021508.

40. Lee, K.-H., Choi, C.-S., and Jeon, K.-S. (2002). Fluorescence tuning using conjugated aromatic imine systems. J. Photoscience *9*, 71–74. https://koreascience.kr/article/JAKO200211922385962.page.

41. Yao, J., Wu, W., Liang, W., Feng, Y., Zhou, D., Chruma, J.J., Fukuhara, G., Mori, T., Inoue, Y., and Yang, C. (2017). Temperature-driven planar chirality switching of a pillar[5]arene-based molecular universal joint. Angew. Chem. Int. Ed. Engl. *56*, 6869–6873. https://doi.org/10.1002/anie.201702542.

42. Ogoshi, T., Yamafuji, D., Akutsu, T., Naito, M., and Yamagishi, T.A. (2013). Achiral guest-induced chiroptical changes of a planar-chiral pillar[5]arene containing one π-conjugated unit. Chem. Commun. *49*, 8782–8784. https://doi.org/10.1039/C3CC44672G.

43. Neese, F., Wennmohs, F., Becker, U., and Riplinger, C. (2020). The ORCA quantum chemistry program package. J. Chem. Phys. *152*, 224108. https://doi.org/10.1063/5.0004608.

44. Bannwarth, C., Ehlert, S., and Grimme, S. (2019). GFN2-xTB—an accurate and broadly parametrized self-consistent tight-binding quantum chemical method with multipole electrostatics and density-dependent dispersion contributions. J. Chem. Theory Comput. *15*, 1652–1671. https://doi.org/10.1021/acs.jctc.8b01176.

45. Marenich, A.V., Cramer, C.J., and Truhlar, D.G. (2009). Universal solvation model based on solute electron density and on a continuum model of the solvent defined by the bulk dielectric constant and atomic surface tensions. J. Phys. Chem. B *113*, 6378–6396. https://doi.org/10.1021/jp810292n.

46. Rebek, J., Wattley, R.V., Costello, T., Gadwood, R., and Marshall, L. (1981). Allosteric effects: binding cooperativity in a subunit model. Angew. Chem. Int. Ed. Engl. *20*, 605–606. https://doi.org/10.1002/anie.198106051.

47. Henkelis, J.J., Blackburn, A.K., Dale, E.J., Vermeulen, N.A., Nassar, M.S., and Stoddart, J.F. (2015). Allosteric modulation of substrate binding within a tetracationic molecular receptor. J. Am. Chem. Soc. *137*, 13252–13255. https://doi.org/10.1021/jacs.5b08656.

48. Ma, Y.-L., Ke, H., Valkonen, A., Rissanen, K., and Jiang, W. (2018). Achieving strong positive cooperativity through activating weak non-covalent interactions. Angew. Chem. Int. Ed. Engl. *57*, 709–713. https://doi.org/10.1002/anie.201711077.

49. Talapaneni, S.N., Kim, D., Barin, G., Buyukcakir, O., Je, S.H., and Coskun, A. (2016). Pillar[5]arene based conjugated microporous polymers for propane/methane separation through host–guest complexation. Chem. Mater. *28*, 4460–4466. https://doi.org/10.1021/acs.chemmater.6b01667.

50. Chao, Y., Thikekar, T.U., Fang, W., Chang, R., Xu, J., Ouyang, N., Xu, J., Gao, Y., Guo, M., Zuilhof, H., and Sue, A.C.-H. (2022). Rim-differentiated" pillar[6]arenes. Angew. Chem. Int. Ed. Engl. *61*, e202204589. https://doi.org/10.1002/anie.202204589.